A Multifunction Control Strategy for the Stable Operation of DG Units in Smart Grids

Edris Pouresmaeil, *Member, IEEE*, Majid Mehrasa, and João P. S. Catalão, *Senior Member, IEEE*

***Abstract*—This paper describes the development of a multifunction control strategy for the stable operation of distributed generation (DG) units during the integration with the power grid. The proposed control model is based on direct Lyapunov control (DLC) theory and provides a stable region for the proper operation of DG units during the integration with the power grid. The compensation of instantaneous variations in the reference current components in ac-side and dc-voltage variations in the dc-side of the interfacing system are adequately considered in this control plan, which is the main contribution and novelty of this paper in comparison with previous control strategies. Utilization of the DLC technique in DG technology can confirm the continuous injection of maximum active power in fundamental frequency from the DG source to the power grid, compensating all the reactive power and harmonic current components of grid-connected loads through the integration of DG link into the grid. Application of this concept in smart grids system can guarantee to reduce the stress on the utility grid during the peak of energy demand. Simulation and experimental test results are presented to demonstrate the proficiency and performance of the proposed DLC technique in DG technology.**

***Index Terms*—Direct Lyapunov control (DLC), distributed generation (DG), power management, smart grids.**

NOMENCLATURE

Indices

k & j a, b, c.

Abbreviations

DG	Distributed generation.
DLC	Direct Lyapunov control.
PF	Power factor.
APF	Active power filter.
LPF	Low-pass filter.
VSC	Voltage source converter.
PCC	Point of power coupling.
PI	Proportional-integral.
PLL	Phase locked loop.

Variables

i_{gk}	Grid currents.
i_{lk}	Load currents.
i_{ck}	DG currents.
i_k	Currents of transistors.
i_c	Current of dc capacitor.
i_{dhn}	Load currents in harmonic frequencies.
i_d	Current components d-axis.
i_q	Current components q-axis.
I_{dc}	dc current.
I_{avd}	Instantaneous variation of I_{refd}.
I_{avq}	Instantaneous variation of I_{refq}.
v_{dc}	Voltage at dc side.
V_{gk}	Grid voltage.
v_m	Reference voltage vector at PCC.
v_k	Voltage of each phase at PCC.
v_r	Reference value of dc side voltage.
S_k	Switching of transistors.
S_j	Switching of transistors in each leg.
S_{eqk}	Switching state function.

Parameters

R_c	Equivalent resistance of the ac filter, coupling transformer, and connection cables.
L_c	Equivalent inductance of the ac filter, coupling transformer, and connection cables.
C	dc capacitor.
P_{ref}	Reference active power of DG.
P_{max}	Maximum active power of DG.
Q_c	Reference reactive power of DG.
Q_l	Load reactive power.
ω	Grid angular frequency.
γ	Constant coefficient of switching function in dynamic state operation.
λ	Constant coefficient of switching function in dynamic state operation.
f	Fundamental frequency.
f_c	Cut-off frequency.

Manuscript received November 26, 2013; revised April 11, 2014, August 5, 2014, and October 19, 2014; accepted November 16, 2014. This work was supported in part by FEDER funds (EU) through COMPETE, in part by the Portuguese funds through FCT under Project FCOMP-01-0124-FEDER-020282 (Ref. PTDC/EEA-EEL/118519/2010) and Project PEst-OE/EEI/LA0021/2013, and in part the EU Seventh Framework Programme FP7/2007-2013 under Grant Agreement 309048. Paper no. TSG-00878-2013.

E. Pouresmaeil is with the Centre for Smart Energy Solutions, University of Southern Denmark, Odense DK-5230, Denmark.

M. Mehrasa is with the Young Researchers and Elite Club, Sari Branch, Islamic Azad University, Sari 195-47715, Iran.

J. P. S. Catalão is with the University of Beira Interior, Covilha 6201-001, Portugal; with the INESC-ID, Lisbon 1000-029, Portugal; and also with the IST, University of Lisbon, Lisbon 1049-001, Portugal (e-mail: catalao@ubi.pt).

Color versions of one or more of the figures in this paper are available online at http://ieeexplore.ieee.org.

Digital Object Identifier 10.1109/TSG.2014.2371991

I. Introduction

THE CONCEPT of DG consists of relatively small generation units which are located at or near the point of power consumption [1]. Application of DG technology in power systems can yield many benefits from both grid and demand sides [2], [3].

DG has the capability of being less costly, highly efficient, and reliable, and it can simplify the generation of energy near the load center [4], [5]. Therefore, DG can be considered as an efficient preference for the residential, commercial, and industrial customer loads to provide a secure and low cost electricity [6], [7], and also multiple integrated DGs can be used to ensure power quality and to provide energy surety to critical loads [8].

Renewable-based energy sources are good options to empower the interfacing system in DG platforms. These sources of energy meet both the decreasing energy demand from the utility grid and the reduction of greenhouse gas emissions for environmental regulations [9], [10].

Power injection from the DG to the grid during the peak of demand can optimize the energy consumption and reduce the stress from the grid's point of view, decreasing also the cost of energy consumption from the customer's point of view [11], [12]. But, increasing the number of DG units in the power grid can introduce some problems in the operation and management of the entire power network [13]. Therefore, an intelligent control technique of DG units for power coordination between the grid, load, and DG sides is highly required in smart grid systems.

Several studies have been reported in the literature regarding the control of the DG interfacing system for integration of renewable and nonrenewable energy sources into the power grid [14]–[19].

For instance, a control technique of multilevel converter topologies for the integration of renewable energy to the grid has been proposed in [20]. The application of this control technique is mainly regarding the injection of harmonic current components and reactive power compensation of nonlinear loads through a source of renewable energy, in medium and high-power systems. Also, supervisory power management has been proposed to control the transitions and to minimize the transients on voltage and frequency of DGs [21].

Different hardware implementations for DG technology, control structures for the interfacing system, and control strategies under fault conditions were addressed in [22].

A control algorithm has been proposed in [23] for reference current generation in the control circuit loop of the interfaced converter in a DG system, under the grid fault condition. The generated reference current components can provide a flexible voltage support during the presence of any faults in the grid voltage.

A PLL-less control technique is presented in [24] for the integration of DG sources into the distribution power grid. By the elimination of PLL from the control loop of DG, synchronization problems between the DG link and power grid can be solved.

In addition, the control loop has a faster dynamic response to the load changes and variations in grid parameters. Performance of this control scheme in DG technology is validated through simulation and experimental test results during transient and steady-state operating conditions. Seamless transfer of single phase interfaced converters between grid-connected and stand-alone modes is introduced in [25]. The proposed strategy is a stable control plan for a single-phase converter which works on a stand-alone and grid connected mode, simultaneously.

Some other control schemes have also been proposed for achieving a unity PF in the utility grid, by the integration of DG sources to the power grid [26], [27].

Pouresmaeil *et al.* [28] presented a feedback linearization technique for the control of a neutral-point-clamped converter for the compensation of harmonic current components of grid-connected loads. By using this control technique, a considerable amount of load currents in harmonic frequencies can be compensated via the DG link; then, total injected power from the utility grid to the load will be free of reactive power and harmonic frequencies. By the introduction of this control method, DG technology can also be considered as an APF device in a typical power system.

Several other control techniques have been proposed in this concept, which in most of the presented studies a solution for a serious problem in the power network has been proposed and discussed [29].

In this paper, the authors are introducing a multifunction control strategy based on the DLC technique, for a stable operation of the proposed model and the VSC control as the heart of the interfacing system between DG sources and the power grid.

The impacts of instantaneous variable variations in the operation of DG systems are adequately considered in the proposed control plan, which is a new contribution of this control method in comparison with other existing strategies.

Indeed, the contribution of this strategy in DG systems can be introduced as a new solution in the distribution grid, while compensating for the different issues needed concurrently during the connection of nonlinear loads to the utility grid.

The rest of this paper is organized into four sections. Following the introduction, the general schematic diagram of the proposed DG model will be introduced in Section II and the dynamic and steady-state analysis of this model will be elaborated. Application of DLC technique for the control and stable operation of the DG interfacing system will be presented in Section III. Moreover, simulation and experimental test results have been performed to demonstrate the efficiency and applicability of the developed control strategy in Section IV. Finally, the conclusions are drawn in Section V.

II. Proposed Model

Fig. 1 shows the general representation of the proposed model, which is based on three main parts, i.e., grid, load, and DG link. Contractual sign of components and variables such as currents and voltages in each phase are illustrated properly in these three sections. Furthermore, the DG source and other components are demonstrated in dc side of interfacing system for empowering it and power injection to the utility grid.

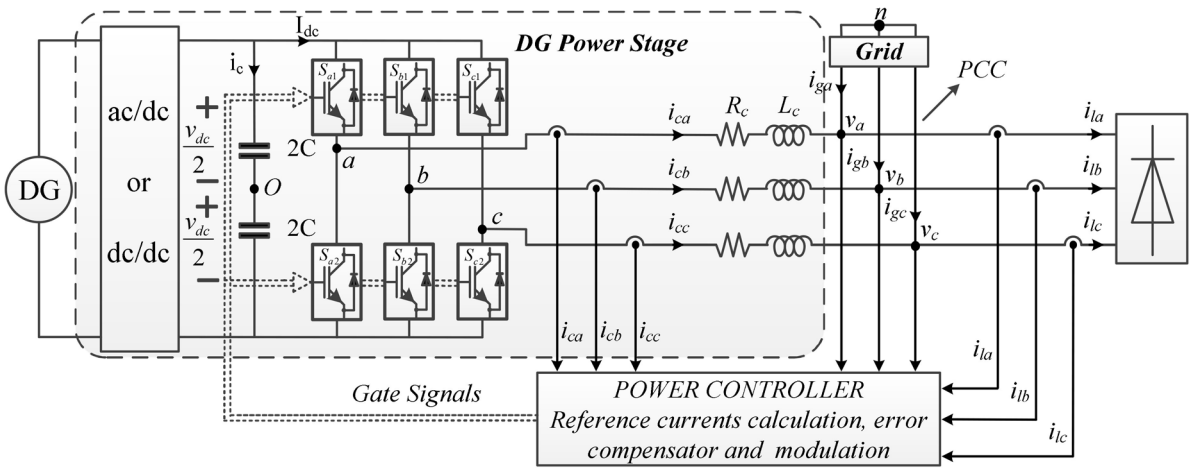

Fig. 1. General schematic diagram of the proposed model.

A. Dynamic State Analysis of the Proposed Model

For designing an applicable control scheme for the interfacing system, the dynamic state of the whole model should be evaluated precisely. By the application of the Kirchhoff's voltage and current laws in both ac and dc sides of the interfaced converter, a general equation of the model can be obtained as

$$L_c \frac{di_{ck}}{dt} + R_c i_{ck} + v_{mk} + v_{kn} = 0 \tag{1}$$

$$C_{\rm dc} \frac{dv_{\rm dc}}{dt} = -\frac{1}{2} \sum_{k=a}^{b,c} \left(S_k - \frac{1}{3} \sum_{j=a}^{b,c} S_j \right) i_k + i_{\rm dc} \tag{2}$$

where $v_{kn} = v_{ko} - v_{no}$. By referring to Fig. 1, the voltage relations between ac and dc sides of the interfacing system can be mentioned as

$$v_{kn} = \frac{v_{\rm dc}}{2} \left(S_k - \frac{1}{3} \sum_{k=a}^{b,c} S_k \right). \tag{3}$$

By substituting (3) in (1), a set of equations for the dynamic behavior of the proposed model in Fig. 1 can be obtained, which is based on the switching state function of the interfaced converter as

$$L_c \frac{di_{ck}}{dt} + R_c i_{ck} - \frac{1}{2} \left(S_k - \frac{1}{3} \sum_{j=a}^{b,c} S_j \right) v_{\rm dc} + v_{mk} = 0. \tag{4}$$

By considering S_{eq} as the switching state function, general dynamic equations for the ac and dc sides of the interfacing system can be expressed as

$$L_c \frac{di_{ck}}{dt} + R_c i_{ck} + S_{\rm eqk} v_{\rm dc} + v_{mk} = 0 \tag{5}$$

$$C_{\rm dc} \frac{dv_{\rm dc}}{dt} - S_{eqa} i_{ca} - S_{eqb} i_{cb} - S_{eqc} i_{cc} - i_{\rm dc} = 0. \tag{6}$$

Equations (5) and (6) describe the behavior of the proposed DG model during the integration time with power grid.

B. Steady-State Analysis of the Proposed Model

Dynamic state equations in (5) and (6) can be transformed into the *dq* reference frame by using the Park transformation matrix, which rotates at the grid angular frequency. By this technique, all the alternative variables of Fig. 1 in fundamental frequency are converted to the dc values; then, filtering and controlling in the control loop of the model can be achieved easier.

Accordingly, the general state space equations of the proposed model can be expressed as

$$L_c \frac{di_{\rm cd}}{dt} + R_c i_{\rm cd} - \omega L_c i_{cq} + S_{\rm eqd} v_{\rm dc} + v_{md} = 0 \tag{7}$$

$$L_c \frac{di_{cq}}{dt} + R_c i_{cq} + \omega L_c i_{\rm cd} + S_{\rm eqq} v_{\rm dc} + v_{mq} = 0 \tag{8}$$

$$C_{\rm dc} \frac{dv_{\rm dc}}{dt} - S_{\rm eqd} i_{\rm cd} - S_{\rm eqq} i_{cq} - i_{\rm dc} = 0. \tag{9}$$

By considering the direction of the reference vector of grid voltage in direction of d-axis, the q-component of grid voltage will be zero ($v_{mq} = 0$) and reference voltage value will be equal to d-component of grid voltage ($v_m = v_{md}$). Assuming $I_{\rm refd}$ as the reference value of d-axis in current control loop of DG for injection of active power to the grid ($I_{\rm cd} = I_{\rm refd}$), and since that in rotating synchronous reference frame q-component of load current is perpendicular on d-component of voltage, $I_{\rm refq}$ will be the reference current of q-axis in DG current control loop, which provides the required reactive power for the loads in both fundamental and harmonic frequencies ($I_{cq} = I_{\rm refq}$). The mentioned assumptions are considered as the stability criteria in the proposed model and by substituting these assumptions in (7)–(9), and considering v_r as the desired value of $v_{\rm dc}$ and $S_{\rm eqds}$ and $S_{\rm eqqs}$ as the switching state values during the steady-state operating condition, a set of equations can be achieved for the steady-state operation of the proposed model as

$$L_c \frac{dI_{\rm refd}}{dt} + R_c I_{\rm refd} - \omega L_c I_{\rm refq} + S_{\rm eqds} v_r + v_m = 0 \tag{10}$$

$$L_c \frac{dI_{\rm refq}}{dt} + R_c I_{\rm refq} + \omega L_c I_{\rm refd} + S_{\rm eqqs} v_r = 0 \tag{11}$$

$$S_{\rm eqds} I_{\rm refd} + S_{\rm eqqs} I_{\rm refq} + I_{\rm dc} = 0. \tag{12}$$

The impacts of instantaneous variations in the values of reference current components should be considered in the control loop of DG to meet an appropriate compensation during the

changes from dynamic to steady-state operating conditions. Consequently

$$\frac{dI_{\text{refd}}}{dt} = I_{\text{avd}}, \frac{dI_{\text{refq}}}{dt} = I_{\text{avq}}. \tag{13}$$

By substituting (13) in (10) and (11), the switching state functions of the interfacing system from the dynamic to the steady-state operating conditions can be expressed as

$$S_{\text{eqds}} = \frac{-v_m - R_c I_{\text{refd}} + \omega L_c I_{\text{refq}} - L_c I_{\text{avd}}}{v_r} \tag{14}$$

$$S_{\text{eqqs}} = \frac{-R_c I_{\text{refq}} - \omega L_c I_{\text{refd}} - L_c I_{\text{avq}}}{v_r}. \tag{15}$$

By substituting the obtained switching state functions in (12), (16) can be achieved as

$$\left(I_{\text{refd}} + \frac{L_c I_{\text{avd}} + v_m}{2R_c}\right)^2 + \left(I_{\text{refq}} + \frac{L_c I_{\text{avq}}}{2R_c}\right)^2 = \frac{(L_c I_{\text{avd}} + v_m)^2 + \left(L_c I_{\text{avq}}\right)^2 + 4R_c v_r I_{\text{dc}}}{4R_c^2} \tag{16}$$

where (16) is the mathematical model for a circle with the center of $((-L_c I_{\text{avd}} - v_m)/2R_c, (-L_c I_{\text{avq}})/2R_c)$ and radius of $\sqrt{((L_c I_{\text{avd}} + v_m)^2 + (L_c I_{\text{avq}})^2 + 4R_c v_r I_{\text{dc}})/(4R_c^2)}$, clarifying the maximum capacity of DG interfacing system for the compensation of active and reactive power components in both dc and alternative frequencies, as another contribution to earlier studies. Fig. 2 shows the comparison between DG and load current components, which clarifies the regions that DG can cover during the connection of nonlinear loads to the grid. As shown in this figure, DG can only supply the load currents that are inside the circle and it is equal to the maximum capacity of the interfacing system for power injection.

Therefore, by considering $i_{cq} = i_{lq}$ and $i_{\text{cd}} = -(L_c I_{\text{avd}} + v_m)/2R_c + \sqrt{\frac{(L_c I_{\text{avd}} + v_m)^2 + (L_c I_{\text{avq}})^2 + 4R_c v_r I_{\text{dc}}}{4R_c^2} - \left(i_{lq} + \frac{L_c I_{\text{avq}}}{2R_c}\right)^2}$ in the control loop of the proposed DG model, the maximum power will be injected from DG to the grid, which is given by the maximum active power and all the reactive power in fundamental frequency, and all the harmonic current components of grid-connected loads.

III. DLC Technique Representation

DLC strategy is considered for the interfacing system control in the control loop of the model represented in Fig. 1. DLC strategy is basically a nonlinear control theory without linearizing the nonlinearities in parameters of the equivalent mathematical system model, bringing a global asymptotic stability for the proposed model [29], [30].

The scalar function in (17) is a general function for DLC technique, which is determined to validate the stability of the proposed model during DG interconnection into the power grid and parameter changes in the whole system

$$H(x_1, x_2, x_3) = \frac{1}{2}L_c x_1^2 + \frac{1}{2}L_c x_2^2 + \frac{1}{2}C x_3^2. \tag{17}$$

Variables x_1 and x_2 clarify the differences between the reference and DG current components in dq frame, and x_3 shows

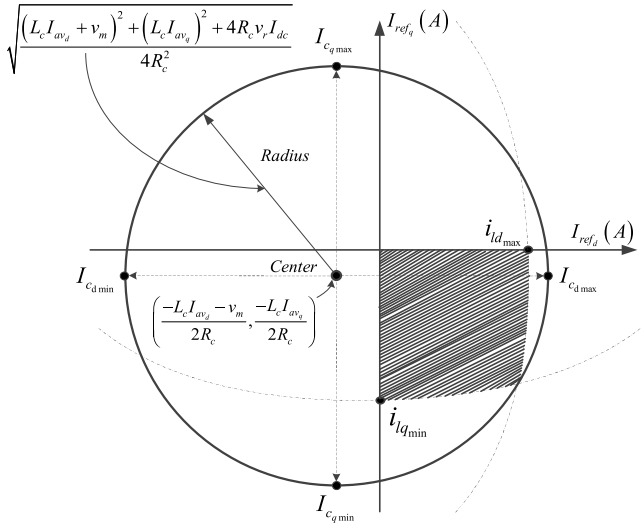

Fig. 2. Comparison between the load and DG current components.

the difference between the dc-voltage generated by DG source and reference voltage value required for the dc-side of interfaced VSC. In addition, (17) demonstrates the total energy of the whole system in the controlled region, which should be dissipated for system stability. To reach this goal, (17) should fulfill the following criteria:

$$\frac{d}{dt}H(x_1, x_2, x_3) = L_c x_1 \frac{dx_1}{dt} + L_c x_2 \frac{dx_2}{dt} + C x_3 \frac{dx_3}{dt} < 0. \tag{18}$$

In order to guarantee a multifunction control technique for reaching a stable operating region for DG units during changes in the parameters of the whole system, the switching state functions of interfaced VSC in the proposed model should be defined as

$$S_{\text{eqd}} = S_{\text{eqds}} + \Delta S_{\text{eqd}} \tag{19}$$

$$S_{\text{eqq}} = S_{\text{eqqs}} + \Delta S_{\text{eqq}}. \tag{20}$$

By substituting (14) and (15) in (7) and (8), time variable parts of (18) can be expanded as

$$L_c \frac{dx_1}{dt} = -R_c i_{\text{cd}} + \omega L_c i_{cq} - L_c I_{\text{avd}} - v_{\text{dc}} \Delta S_{\text{eqd}} - v_{\text{dc}} \left(\frac{\omega L_c I_{\text{refq}} - R_c I_{\text{refd}} - L_c I_{\text{avd}} - v_m}{v_r}\right) - v_m \tag{21}$$

$$L_c \frac{dx_2}{dt} = -R_c i_{cq} - \omega L_c i_{\text{cd}} - L_c I_{\text{avq}} - v_{\text{dc}} \Delta S_{\text{eqq}} - v_{\text{dc}} \left(\frac{-\omega L_c I_{\text{refd}} - R_c I_{\text{refq}} - L_c I_{\text{avq}}}{v_r}\right) \tag{22}$$

$$C \frac{dx_3}{dt} = \left(\frac{-v_m + \omega L_c I_{\text{refq}} - R_c I_{\text{refd}} - L_c I_{\text{avd}}}{v_r}\right) i_{\text{cd}} + \left(\frac{-\omega L_c I_{\text{refd}} - R_c I_{\text{refq}} - L_c I_{\text{avq}}}{v_r}\right) i_{cq} + \Delta S_{\text{eqd}} i_{\text{cd}} + \Delta S_{\text{eqq}} i_{cq} + i_{\text{dc}} - \left(S_{\text{eqds}} I_{\text{refd}} + S_{\text{eqqs}} I_{\text{refq}} + I_{\text{dc}}\right). \tag{23}$$

Moreover, by substituting $x_1 = i_{\text{cd}} - I_{\text{refd}}$, $x_2 = i_{cq} - I_{\text{refq}}$, $x_3 = v_{\text{dc}} - v_r$, (21)–(23) in (18), and considering the definitions

in (13), (24) can be obtained as

$$\begin{aligned}\frac{d}{dt}H(x_1,x_2,x_3) = &-R_c(i_{\rm cd}-I_{\rm refd})^2 - R_c\left(i_{cq}-I_{\rm refq}\right)^2\\ &-\Delta S_{\rm eqd}\left(v_r i_{\rm cd}-v_{\rm dc}I_{\rm refd}\right)\\ &-\Delta S_{\rm eqq}\left(v_r i_{cq}-v_{\rm dc}I_{\rm refq}\right)\\ &-\left(v_{\rm dc}-v_r\right)\left(i_{\rm dc}-I_{\rm dc}\right).\end{aligned}\tag{24}$$

Equation (24) should have a negative value to meet the stability criteria during operation of the proposed DG model in a smart grid system. To reach this goal, all the terms in (24) should be analyzed properly one-by-one. It is clear that the first and second terms of this equation have negative values; moreover, the switching state functions of the interfacing system can be defined to have a positive definite total energy and a flexible reflection against the dynamic changes by considering $\Delta S_{\rm eqd}$ and $\Delta S_{\rm eqq}$ as

$$\Delta S_{\rm eqd} = \gamma\left(v_r i_{\rm cd}-v_{\rm dc}I_{\rm refd}\right)\tag{25}$$

$$\Delta S_{\rm eqq} = \lambda\left(v_r i_{cq}-v_{\rm dc}I_{\rm refq}\right).\tag{26}$$

Furthermore, $v_{\rm dc}$ tends to be equal to v_r for making an appropriate compatibility between the voltage of dc and ac sides during the integration time. It happens during the steady-state operating condition; then, the last term in (24) will be eliminated and consequently the value of the general equation will be negative during the steady state. But, during the transient time, two conditions and values can be expected for $v_{\rm dc}$ in comparison with v_r.

At first condition, the value of $v_{\rm dc}$ can be less than v_r; then if

$$v_{\rm dc} < v_r \rightarrow i_{\rm dc} < I_{\rm dc}$$

then

$$\left(v_{\rm dc}-v_r\right) < 0 \quad \text{and} \quad \left(i_{\rm dc}-I_{\rm dc}\right) < 0$$

therefore

$$-\left(v_{\rm dc}-v_r\right)\left(i_{\rm dc}-I_{\rm dc}\right) < 0.\tag{27}$$

At second condition, the $v_{\rm dc}$ value can be greater than v_r; then if

$$v_{\rm dc} > v_r \rightarrow i_{\rm dc} > I_{\rm dc}$$

then

$$\left(v_{\rm dc}-v_r\right) > 0 \quad \text{and} \quad \left(i_{\rm dc}-I_{\rm dc}\right) > 0$$

therefore

$$-\left(v_{\rm dc}-v_r\right)\left(i_{\rm dc}-I_{\rm dc}\right) < 0.\tag{28}$$

Based on (25)–(28), we can write the following upper bound on $\dot{H}(x_1,x_2,x_3)$:

$$\begin{aligned}\frac{d}{dt}H_{\rm leq}(x_1,x_2,x_3) = &-R_c(i_{\rm cd}-I_{\rm refd})^2 - R_c\left(i_{cq}-I_{\rm refq}\right)^2\\ &-\gamma\left(v_r i_{\rm cd}-v_{\rm dc}I_{\rm refd}\right)^2\\ &-\lambda\left(v_r i_{cq}-v_{\rm dc}I_{\rm refq}\right)^2\end{aligned}\tag{29}$$

which by LaSalle–Yoshizawa [31], we can conclude that the vector of the tracking errors $[x_1\ x_2\ x_3]$ converges asymptotically to zero.

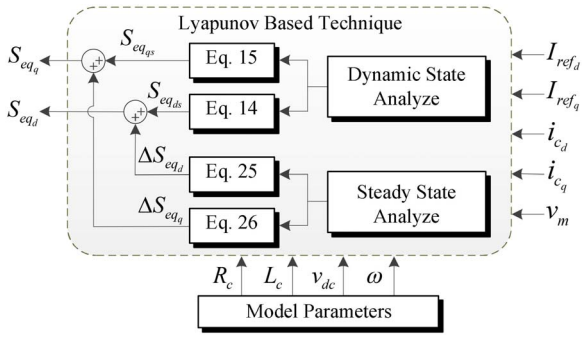

Fig. 3. Control block diagram of the interfacing system in the proposed model.

As a result, application of DLC technique can guarantee a stable operation for the proposed DG model during both dynamic and steady state operating conditions.

Fig. 3 shows the control block diagram of the proposed model based on DLC technique.

The proposed control strategy which combines (14), (15), (25), and (26) can create a global asymptotic stable region for the DG operating areas.

A. Stability Analysis of DC-Link Voltage

The stable operation of the interfaced converter is highly dependent on an appropriate adjustment between the dc-link voltage and voltage of ac grid. Dynamic analysis of dc-link voltage is investigated precisely in this section in order to verify the stability and performance of the proposed DG model based on DLC technique.

The switching state functions of interfaced converter of DG unit can be obtained from (7) and (8) in both the dynamic and steady-state operating conditions as

$$S_{\rm eqd} = \frac{-1}{v_{\rm dc}}\left(L_c\frac{di_{\rm cd}}{dt} + R_c i_{\rm cd} - \omega L_c i_{cq} + v_{md}\right)\tag{30}$$

$$S_{\rm eqq} = \frac{-1}{v_{\rm dc}}\left(L_c\frac{di_{cq}}{dt} + R_c i_{cq} + \omega L_c i_{\rm cd}\right).\tag{31}$$

The dynamic equation of dc-link voltage can be achieved by substituting (30) and (31) in (9) as

$$\frac{dv_{\rm dc}}{dt} = \frac{i_{\rm dc}}{C_{\rm dc}} - \frac{L_c i_{\rm cd}\frac{di_{\rm cd}}{dt} + R_c i_{\rm cd}^2 + i_{\rm cd}v_{md} + L_c i_{cq}\frac{di_{cq}}{dt} + R_c i_{cq}^2}{C_{\rm dc}v_{\rm dc}}.\tag{32}$$

The zero dynamic of dc-link voltage can be obtained by imposing zero into the changes in dc-link voltage as $(dv_{\rm dc})/dt = 0$. Therefore, the value of dc-link voltage for a stable operation of the interfaced converter during the integration time with ac grid can be expressed as

$$v_{\rm dc} = \frac{L_c i_{\rm cd}\frac{di_{\rm cd}}{dt} + L_c i_{cq}\frac{di_{cq}}{dt} + R_c i_{\rm cd}^2 + R_c i_{cq}^2 + i_{\rm cd}v_{md}}{i_{\rm dc}}.\tag{33}$$

Equation (33) describes a zero dynamic change in dc-link voltage of DG unit and can be written as

$$\left(L_c i_{\rm cd}\frac{di_{\rm cd}}{dt} + L_c i_{cq}\frac{di_{cq}}{dt} + R_c\left(i_{\rm cd}^2 + i_{cq}^2\right)\right) + i_{\rm cd}v_{md} = v_{\rm dc}i_{\rm dc}.\tag{34}$$

Equation (34) demonstrates that the input power of DG unit is consumed to generate dissipated and reserved power in output resistance and inductance of the DG unit. The remaining input power will be injected to the utility grid through the DG link. In addition, (34) verifies that the dc-link voltage in the obtained dynamic model is equal to a constant value. In order to prove the dc voltage convergence to its desired value, the error of dynamic changes in dc-link voltage should be precisely analyzed.

With respect to (23), (35) can be obtained as

$$C\frac{dx_3}{dt} = S_{\text{eqds}}x_1 + S_{\text{eqqs}}x_2 + \Delta S_{\text{eqd}}i_{\text{cd}} + \Delta S_{\text{eqq}}i_{cq} + (i_{\text{dc}} - I_{\text{dc}}). \quad (35)$$

The proposed control loop should be able to follow the reference current components in *d-q* frame with a fast dynamic response during the load changes ($i_{\text{cd}} \rightarrow I_{\text{refd}}$ and $i_{cq} \rightarrow I_{\text{refq}}$). Therefore, by referring to (35), the error value in the dynamic model of dc-link voltage can be achieved as

$$\frac{dx_3}{dt} = \frac{1}{C}\left(\gamma I_{\text{refd}}^2 + \lambda I_{\text{refq}}^2\right)x_3 + \frac{1}{C}(i_{\text{dc}} - I_{\text{dc}}). \quad (36)$$

The zero dynamic of dc voltage error is calculated by $(dx_3)/dt = 0$; then

$$x_3 = -\frac{(i_{\text{dc}} - I_{\text{dc}})}{\gamma I_{\text{refd}}^2 + \lambda I_{\text{refq}}^2}. \quad (37)$$

Equation (37) illustrates that the specified values of reference currents in the control loop of DG unit, and constant coefficients of switching functions with small changes in dc input current, lead to a stable and zero dynamic value for dc voltage error ($x_3 = 0$).

B. Reference Current Calculation

Current reference values should be defined based on the objectives of the DLC strategy for an efficient operation of DG during the dynamic and steady-state operating conditions. Therefore, injection of all the harmonic current components, maximum active power, and all the reactive power should be considered in the control loop of DG model. By this consideration and based on Fig. 2, the remaining power during connection of additional load, which will be supplied through the utility grid, will be an active power in reference frequency.

Based on the mentioned assumptions, d-component value of reference current in the control loop of the proposed model will be achieved by the sum of the maximum capacity of DG interfacing system for injection of active power in main frequency and alternative terms of load current components in d-axis as

$$i_{\text{cd}}^* = \frac{P_{\max}}{v_m} + \sum_{n=2}^{\infty} i_{\text{dhn}} = \frac{P_{\text{ref}}}{v_m} + i_{ld}(1 - \text{LPF}). \quad (38)$$

The alternative parts of load current can be separated from the dc part by a LPF. The considered filter has a cut-off frequency $f_c = (f/2)$ ($f = 50$Hz), which promises the extraction of the dc part from the nonlinear load currents. Furthermore,

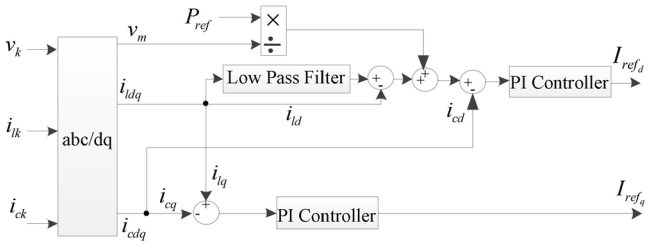

Fig. 4. Reference current generator.

to compensate the reactive power of the load at fundamental and harmonic frequencies, DG must inject i_{lq} as

$$i_{\text{cd}}^* = -\frac{Q_C}{v_m} = -\frac{Q_l}{v_m} = i_{lq}. \quad (39)$$

The difference between the DG and reference currents should be passed through a PI controller in order to obtain a fast dynamic response and high accuracy to track and provide the load current components in steady-state condition and to reduce the current overshoot during integration time between the grid and DG. Fig. 4 shows the block diagram of reference currents calculation.

IV. Results and Discussion

Simulation and experimental test results will be presented in this section in order to confirm the high performance of DLC technique for the control of VSC as the interfacing system between the dispersed energy sources and the main grid.

The complete model was simulated by MATLAB/Simulink in "Power System Block set" and validated through experimental test results. The proposed methodology is implemented using Texas Instruments TMS320F2808 fixed-point DSP control board for the hardware implementation of DLC method in a real-time system. The overall structure of the simulated model is depicted in Fig. 5, which is composed by the Thévenin model of grid voltage and impedance, grid-connected loads, and DG model including DLC scheme.

Parameter values for the simulated model are presented in Table I. In addition, the hardware implementation structure, which is equivalent to the simulated model of Fig. 5 is shown in Fig. 6. The parameters are defined in Table II.

As illustrated in Fig. 5, a nonlinear load is connected to the utility grid before connection of DG link, drawing the current components in both the dc and harmonic frequencies from the grid, continuously. This operation is continued up to $t = 0.1$ s at which time DG is integrated to the grid and starts to inject the available power from the dispersed energy sources to the grid based on the defined objectives in the control loop of the model. This procedure is continued up to $t = 0.2$ s at which a secondary nonlinear load analogous to the first load is added to the first load. In this condition, the total power of the two loads is more than the maximum capacity of DG ($S_{\text{DG}} < S_{\text{load}}$).

Fig. 7 indicates the simulation results for the load, grid, and DG currents during these three operating times. As depicted

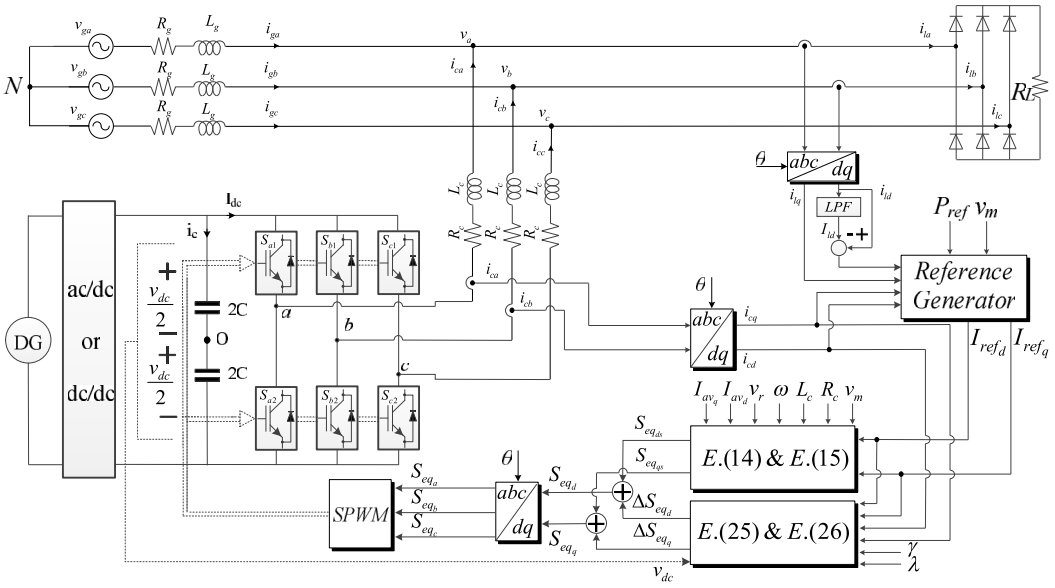

Fig. 5. General structure of the model and control block diagram.

TABLE I
SIMULATION MODEL PARAMETERS

Parameter	*Value*
Grid voltage	380 V
dc-link voltage set-point (v_{dc})	800 V
Fundamental frequency	50 Hz
Switching/Sampling frequency	10 kHz
Converter resistance	0.1 mΩ
Converter inductance	0.45 mH
γ	0.001
λ	0.0001
Reference power of DG	6.5 kW

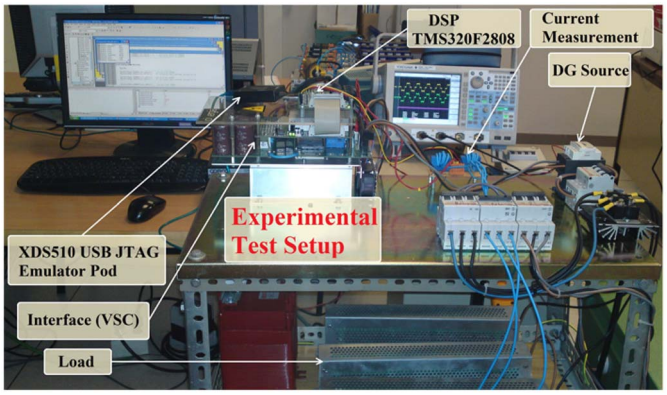

Fig. 6. Experimental test set-up for the proposed DG model.

TABLE II
EXPERIMENTAL SETUP PARAMETERS

Parameter	*Value*
Grid voltage	80 V
dc-link voltage set-point (v_{dc})	250 V
dc-link capacitance	1020 μF
Fundamental frequency	50 Hz
Switching/Sampling frequency	5 kHz
Nonlinear load resistance	30 Ω
Interfacing inductance	0.46 mH

in this figure, during $0.1 < t$ (s) < 0.2 all the load current components in both the dc and harmonic frequencies are supplied trough the DG and injected power from the utility grid to the load reduced to the zero value ($S_{\text{load}} < S_{\text{DG}}$).

But, while the second load is added up to the first load during $0.2 < t$ (s) < 0.3, the maximum injected power from the DG to the grid is less than the required power for supplying the loads; then, the remaining power is compensated through the grid side. As shown in this figure, the injected current via the grid to the load is sinusoidal and free of harmonic frequencies during the load increment.

The same scenario has been repeated in the experimental test bench and the result is depicted in Fig. 8, for the time prior and after the second load increment.

As shown in this figure, all the load current components in both the main and alternative frequencies are supplied through the DG link before the load increment, then the grid current is reduced to the zero value.

However, after the second load is added to the first load, DG injects the maximum available power to supply the loads, since this value is less than all the requested power from the load side; then, the rest of the power, which is active power in the main frequency, is injected via the grid side.

Fig. 9 shows the simulation results of load voltage and grid current during the connection of the secondary load to the grid.

As shown in this figure, the grid current and load voltage are in phase, confirming the capability of the DLC technique for the injection of reactive power from DG to supply the

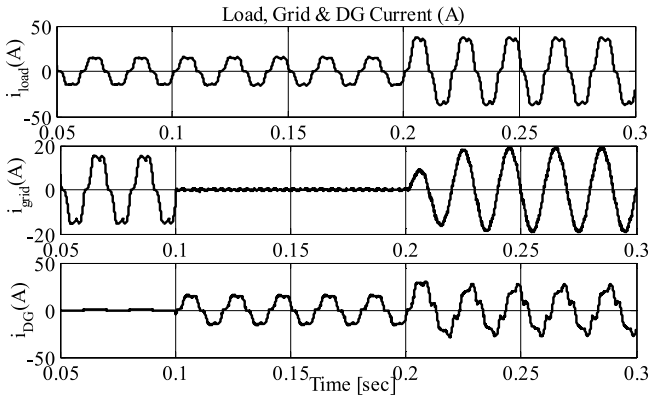

Fig. 7. Load, grid, and DG currents before and after DG integration to the grid, and before and after the second load increment.

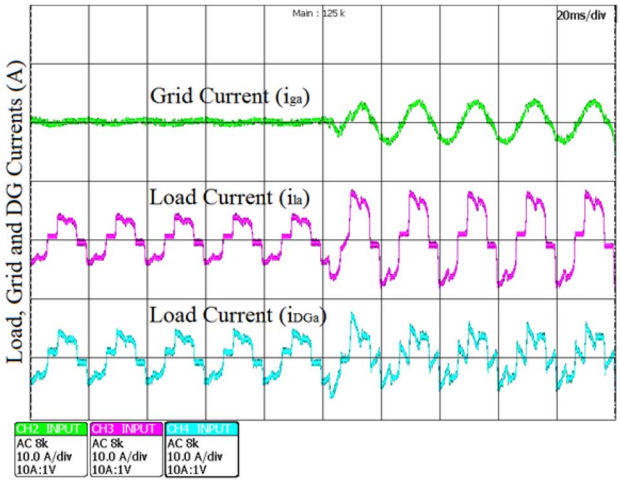

Fig. 8. Experimental test result of load, grid, and DG currents before and after the additional load increment.

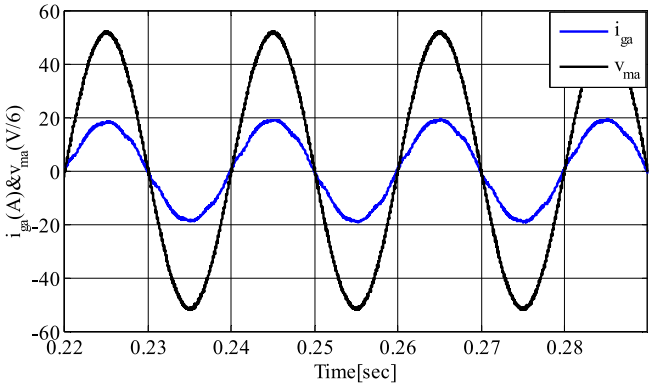

Fig. 9. Load voltage and grid current during the additional load increment.

load. In other words, after connection of the second load to the first load, DG injects the maximum active power in grid frequency, which is based on the reference power definition, all the harmonic current components in d and q-axis and all the reactive power of the loads in main frequency.

Therefore, injected currents from the grid to the load will be free of harmonic frequencies and reactive power components.

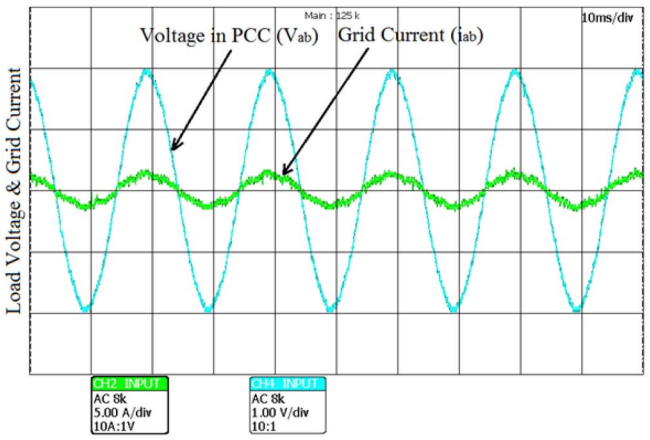

Fig. 10. Experimental test result of load voltage and grid current during the additional load increment.

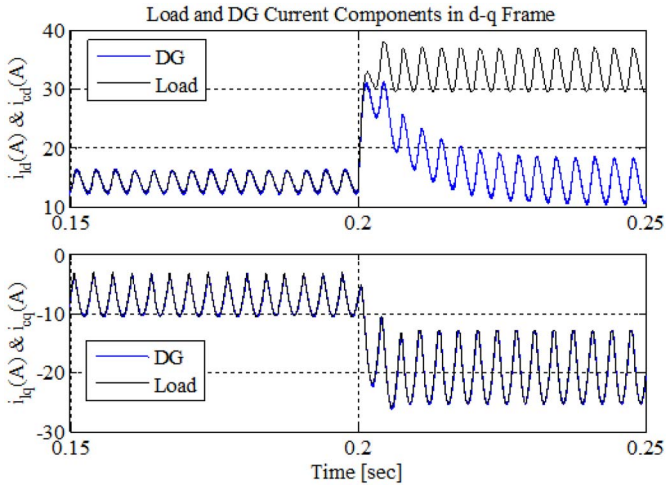

Fig. 11. Dynamic response of DG link in tracking the load current components in DLC control loop before and after additional load increment.

Fig. 10 indicates the same figure as Fig. 9 to validate the ability of the proposed DG model for compensating harmonic current components and reactive power of nonlinear loads through the experimental test results.

Accordingly, besides the active power injection from DG source to the grid, the DLC technique introduces the DG as APF and PF correction devices in the power system.

The capability of the DLC technique for tracking the reference current components in the control loop of the DG system is validated by simulation and experimental results in Figs. 11 and 12, respectively, for the duration before and after the connection of the second load to the grid.

These figures confirm that the control loop of DG follows all the reference current components with a fast and accurate dynamic response, and also demonstrate that after the load increment DG injects the maximum active power based on the maximum capacity of the interfaced converter, all the harmonic current components in d and q-axis and all the reactive power required to supply the loads, reaching the unity PF in the utility grid.

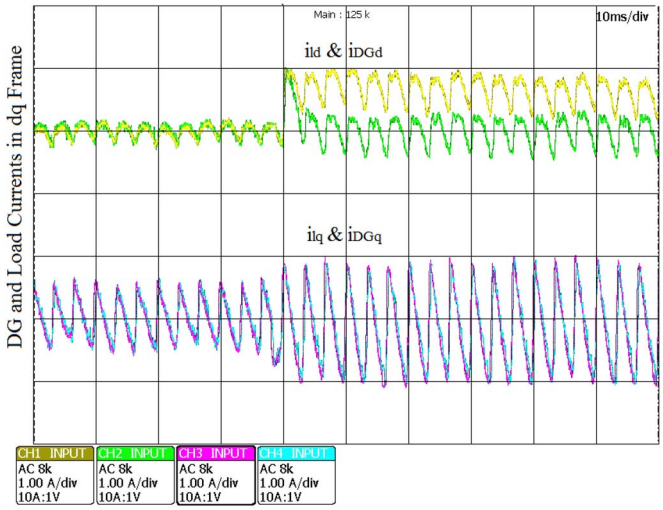

Fig. 12. Experimental test result to confirm the fast dynamic response of DG link for tracking the load current components in the DLC control loop, before and after the additional load increment.

V. Conclusion

A control plan based on DLC method has been developed for the integration of DG sources to the grid. The main objective of the proposed control technique was to prepare a secure and low cost energy for the loads from the dispersed sources of energy, specially based on the renewable energy sources. The main advantage of our proposed control technique over the other control techniques was its high performance for the compensation of active and reactive power changes and harmonic current components of nonlinear loads. By the utilization of the DLC technique, DG can provide continuous injection of maximum active power in grid frequency, all the reactive power and harmonic current components of grid-connected loads, via connection of distributed energy resources into the power grid. The proper application of this technique in a smart grid system can reduce the stress on the utility grid by injection of power from the DG source into the grid during the peak of demand, which can also decrease the cost of consumed energy from the customer's point of view. The high performance of DLC technique has been validated through simulation and experimental test results during both dynamic and steady-state operating conditions, certifying the concept of DLC method as a multifunction control technique in DG technology, which is very important for the proper operation of sensitive loads in the power grid.

References

[1] F. H. Guan, D. M. Zhao, X. Zhang, B. T. Shan, and Z. Liu, "Research on distributed generation technologies and its impacts on power system," in *Proc. IEEE Sustain. Power Gener. Supply*, Nanjing, China, 2009, pp. 1–6.

[2] B. P. Hayes, A. J. Collin, J. L. Acosta, and S. Z. Djokic, "Assessment of the influence of distributed generation and demand side management on transmission system performance," in *Proc. 7th Power Gener. Transmiss. Distrib. Energy Convers. (MedPower)*, Agia Napa, Cyprus, 2010, pp. 1–10.

[3] M. F. Akorede, H. Hizam, and E. Pouresmaeil, "Distributed energy resources and benefits to the environment," *Renew. Sustain. Energy Rev.*, vol. 14, no. 2, pp. 724–734, Feb. 2010.

[4] M. F. Shaaban, Y. M. Atwa, and E. F. El-Saadany, "DG allocation for benefit maximization in distribution networks," *IEEE Trans. Power Syst.*, vol. 28, no. 2, pp. 639–649, May 2013.

[5] L. F. Ochoa and G. P. Harrison, "Minimizing energy losses: Optimal accommodation and smart operation of renewable distributed generation," *IEEE Trans. Power Syst.*, vol. 26, no. 1, pp. 198–205, Feb. 2011.

[6] D. Singhand and R. Misra, "Effect of load models in distributed generation planning," *IEEE Trans. Power Syst.*, vol. 22, no. 4, pp. 2204–2212, Nov. 2007.

[7] I. Waseem, M. Pipattanasomporn, and S. Rahman, "Reliability benefits of distributed generation as a backup source," in *Proc. IEEE Power Energy Soc. Gen. Meeting*, Calgary, AB, Canada, 2009, pp. 1–8.

[8] F. Qiang *et al.*, "Microgrid generation capacity design with renewables and energy storage addressing power quality and surety," *IEEE Trans. Smart Grid*, vol. 3, no. 4, pp. 2019–2027, Dec. 2012.

[9] A. Mishra, D. Irwin, P. Shenoy, J. Kurose, and R. Misra, "GreenCharge: Managing renewable energy in smart buildings," *IEEE J. Sel. Areas Commun.*, vol. 31, no. 7, pp. 1281–1293, Jul. 2013.

[10] K. Qian, C. Zhou, Y. Yuan, X. Shi, and M. Allan, "Analysis of the environmental benefits of distributed generation," in *Proc. IEEE Power Energy Soc. Gen. Meeting*, Pittsburgh, PA, USA, 2008, pp. 1–5.

[11] Y. Zhang, N. Gatsis, and G. B. Giannakis, "Robust energy management for microgrids with high-penetration renewables," *IEEE Trans. Sustain. Energy*, vol. 4, no. 4, pp. 944–953, Oct. 2013.

[12] Y. Zhang, M. Mao, M. Ding, and L. Chang, "Study of energy management system for distributed generation systems," in *Proc. IEEE Electr. Util. Deregul. Restruct. Power Technol.*, Nanjing, China, 2008, pp. 2465–2469.

[13] F. Katiraei and M. R. Iravani, "Power management strategies for a microgrid with multiple distributed generation units," *IEEE Trans. Power Syst.*, vol. 21, no. 4, pp. 1821–1831, Nov. 2006.

[14] E. Pouresmaeil, D. Montesinos-Miracle, and O. Gomis-Bellmunt, "Control scheme of three-level NPC inverter for integration of renewable energy resources into AC grid," *IEEE Syst. J.*, vol. 6, no. 2, pp. 242–253, Jun. 2012.

[15] M. Mehrasa, M. E. Adabi, E. Pouresmaeil, and J. Adabi, "Passivity-based control technique for integration of DG resources into the power grid," *Int. J. Elect. Power Energy Syst.*, vol. 58, pp. 281–290, Jun. 2014.

[16] E. J. Coster, J. M. A. Myrzik, B. Kruimer, and W. L. Kling, "Integration issues of distributed generation in distribution grids," *Proc. IEEE*, vol. 99, no. 1, pp. 28–39, Jan. 2011.

[17] Z. Zeng, H. Yang, R. Zhao, and C. Cheng, "Topologies and control strategies of multi-functional grid-connected inverters for power quality enhancement: A comprehensive review," *Renew. Sustain. Energy Rev.*, vol. 24, pp. 223–270, Aug. 2013.

[18] H. Yazdanpanahi, Y. W. Li, and W. Xu, "A new control strategy to mitigate the impact of inverter-based DGs on protection system," *IEEE Trans. Smart Grid*, vol. 3, no. 3, pp. 1427–1436, Sep. 2012.

[19] F. Gao and M. R. Iravani, "A control strategy for a distributed generation unit in grid-connected and autonomous modes of operation," *IEEE Trans. Power Del.*, vol. 23, no. 2, pp. 850–859, Apr. 2008.

[20] E. Pouresmaeil, O. Gomis-Bellmunt, D. Montesinos-Miracle, and J. Bergas-Jane, "Multilevel converters control for renewable energy integration to the power grid," *Energy*, vol. 36, no. 2, pp. 950–963, Feb. 2011.

[21] F. Qiang *et al.*, "Transition management of microgrids with high penetration of renewable energy," *IEEE Trans. Smart Grid*, vol. 5, no. 2, pp. 539–549, Mar. 2014.

[22] F. Blaabjerg, R. Teodorescu, M. Liserre, and A. V. Timbus, "Overview of control and grid synchronization for distributed power generation systems," *IEEE Trans. Power Electron.*, vol. 53, no. 5, pp. 1398–1409, Oct. 2006.

[23] A. Camacho, M. Castilla, J. Miret, J. C. Vasquez, and E. Alarcon-Gallo, "Flexible voltage support control for three-phase distributed generation inverters under grid fault," *IEEE Trans. Ind. Electron.*, vol. 60, no. 4, pp. 1429–1441, Apr. 2013.

[24] E. Pouresmaeil, C. Miguel-Espinar, M. Massot-Campos, D. Montesinos-Miracle, and O. Gomis-Bellmunt, "A control technique for integration of DG units to the electrical networks," *IEEE Trans. Ind. Electron.*, vol. 60, no. 7, pp. 2881–2893, Jul. 2013.

[25] Z. Yao, L. Xiao, and Y. Yan, "Seamless transfer of single-phase grid interactive inverters between grid-connected and stand-alone modes," *IEEE Trans. Power Electron.*, vol. 25, no. 6, pp. 1597–1603, Jun. 2010.

[26] F. D. Freijedo, J. Doval-Gandoy, O. Lopez, and E. Acha, "Tuning of phase locked loops for power converters under distorted utility conditions," *IEEE Trans. Ind. Appl.*, vol. 45, no. 6, pp. 2039–2047, Nov./Dec. 2009.

[27] R. M. S. Filho, P. F. Seixas, P. C. Cortizo, L. A. B. Torres, and A. F. Souza, "Comparison of three single-phase PLL algorithms for UPS applications," *IEEE Trans. Ind. Electron.*, vol. 55, no. 8, pp. 2923–2932, Aug. 2008.
[28] E. Pouresmaeil, D. Montesinos-Miracle, O. Gomis-Bellmunt, and A. Sudria-Andreu, "Instantaneous active and reactive current control technique of shunt active power filter based on the three-level NPC inverter," *Eur. Trans. Elect. Power*, vol. 21, no. 7, pp. 2007–2022, Oct. 2011.
[29] S. Dasgupta, S. N. Mohan, S. K. Sahoo, and S. K. Panda, "Lyapunov function-based current controller to control active and reactive power flow from a renewable energy source to a generalized three-phase microgrid system," *IEEE Trans. Ind. Electron.*, vol. 60, no. 2, pp. 799–813, Feb. 2013.
[30] A. Isidori, *Nonlinear Control Systems*, 2nd ed. Berlin, Germany: Springer-Verlag, 1995.
[31] W. Haddad and V. S. Chellaboina, *Nonlinear Dynamical Systems and Control: A Lyapunov-Based Approach*. Princeton, NJ, USA: Princeton Univ. Press, 2008.

Edris Pouresmaeil (M'14) received the B.Sc. and M.Sc. degrees in electrical engineering from the University of Mazandaran, Babol, Iran, in 2003 and 2005, respectively, and the Ph.D. (Hons.) degree in electrical engineering from the Technical University of Catalonia, Barcelona Tech. (UPC), Barcelona, Spain, in 2012.

He joined the Department of Electrical and Computer Engineering, University of Waterloo, Waterloo, ON, Canada, as a Post-Doctoral Research Fellow, and then joined the Department of Electromechanical Engineering, University of Beira Interior, Covilhã, Portugal. He is currently an Associate Professor with the Centre for Smart Energy Solutions, University of Southern Denmark, Odense, Denmark. His current research interests include power electronics converters for distributed generation, microgrids operation, integration of renewable energies in smart grids, and energy hub management system.

Majid Mehrasa received the B.Sc. and M.Sc. degrees in electrical engineering from the University of Mazandaran, Babol, Iran, in 2006 and 2009, respectively.

He is currently with the Young Researchers and Elite Club, Sari Branch, Islamic Azad University, Sari, Iran. His current research interests include application of nonlinear control theories into multilevel converters, distributed generation, active power filter, and microgrid operation.

João P. S. Catalão (M'04–SM'12) received the M.Sc. degree from the Instituto Superior Técnico, Lisbon, Portugal, in 2003, and the Ph.D. and Habilitation degrees for Full Professor ("Agregação") from the University of Beira Interior (UBI), Covilhã, Portugal, in 2007 and 2013, respectively.

He is currently a Professor with UBI and a Director of the Sustainable Energy Systems Laboratory with INESC-ID. He is the Primary Coordinator of the EU-funded FP7∼Project Smart and Sustainable Insular Electricity Grids Under Large-Scale Renewable Integration, a 5.2 million euro project involving 11 industry partners. His current research interests include power system operations and planning, hydro and thermal scheduling, wind and price forecasting, distributed renewable generation, demand response, and smart grids. He has authored or co-authored over 285 publications, including 95 journal papers, 175 conference proceedings papers, and 12 book chapters. He has edited the book entitled *Electric Power Systems: Advanced Forecasting Techniques and Optimal Generation Scheduling* (CRC Press, 2012), which was translated into Chinese in 2014. He is currently editing another book entitled *Smart and Sustainable Power Systems: Operations, Planning and Economics of Insular Electricity Grids* (CRC Press, 2015).

Prof. Catalão was the recipient of the 2011 Scientific Merit Award UBI-FE/Santander Universities and the 2012 Scientific Award UTL/Santander Totta. He is an Editor of the IEEE TRANSACTIONS ON SMART GRID, the IEEE TRANSACTIONS ON SUSTAINABLE ENERGY, and an Associate Editor of *IET Renewable Power Generation*. He was the Guest Editor-in-Chief for the Special Section on Real-Time Demand Response of the IEEE TRANSACTIONS ON SMART GRID, published in 2012, and is currently a Guest Editor-in-Chief for the Special Section on Reserve and Flexibility for Handling Variability and Uncertainty of Renewable Generation of the IEEE TRANSACTIONS ON SUSTAINABLE ENERGY.